The Astrophysical Journal, 799:109 (9pp), 2015 January 20 doi:10.1088/0004-637X/799/1/109

EVIDENCE FOR AN ANHYDROUS CARBONACEOUS EXTRASOLAR MINOR PLANET

M. Jura[1], P. Dufour[2], S. Xu (许偲艺)[1,3], B. Zuckerman[1], B. Klein[1], E. D. Young[4], and C. Melis[5]
[1] Department of Physics and Astronomy, University of California, Los Angeles, CA 90095-1562, USA; jura@astro.ucla.edu, kleinb@astro.ucla.edu, ben@astro.ucla.edu
[2] Département de Physique, Université de Montréal, Montréal, Québec H3C 3J7, Canada; dufourpa@astro.umontreal.ca
[3] European Southern Observatory (ESO), D-85748 Garching, Germany; sxu@eso.org
[4] Department of Earth, Planetary, and Space Sciences, University of California, Los Angeles, Los Angeles, CA 90095, USA; eyoung@ess.ucla.edu
[5] Center for Astrophysics and Space Sciences, University of California, San Diego, CA 92093-0424, USA; cmelis@ucsd.edu
Received 2014 October 18; accepted 2014 November 17; published 2015 January 20

ABSTRACT

Using Keck/HIRES, we report abundances of 11 different elements heavier than helium in the spectrum of Ton 345, a white dwarf that has accreted one of its own minor planets. This particular extrasolar planetesimal, which was at least 60% as massive as Vesta, appears to have been carbon-rich and water-poor; we suggest it was compositionally similar to those Kuiper Belt Objects with relatively little ice.

Key words: planetary systems – white dwarfs

1. INTRODUCTION

Because of the vagaries of gravitational dynamics that occur within a white dwarf's planetary system, a minor planet's orbit can be strongly perturbed so that it passes close enough to the host star to be tidally disrupted (Debes & Sigurdsson 2002; Bonsor et al. 2011; Veras & Wyatt 2012; Frewen & Hansen 2014). A circumstellar disk is then formed, and the white dwarf ultimately accretes the resulting debris, thereby imparting a signature in the stellar spectrum which would otherwise be essentially pure hydrogen or, less often, pure helium (Jura 2003). By determining the abundances of heavy elements in the atmosphere of the host white dwarf, we can measure the bulk elemental compositions of extrasolar minor planets to investigate their history and evolution and to compare and contrast with solar system bodies (Jura & Young 2014).

Carbon and oxygen are the most abundant heavy elements in planet forming environments. However, they can be carried in volatile molecules and are not automatically incorporated into rocky planetesimals. As a result, many observational and theoretical efforts have been devoted toward understanding the fate of these elements in protoplanetary disks (Bergin 2013; Henning & Semenov 2013). In the simplest standard picture, most oxygen is combined into water and is retained onto solids exterior to the snow line. In these same environments, if interstellar solid carbon grains are destroyed as what occurred within the inner solar system (Lee et al. 2010), most carbon is carried in volatile molecules such as CH_4 and CO_2. Consequently, little carbon accumulates into planetesimals unless they form in an extremely cold environment far from the central star. Therefore, within asteroids, carbon is expected to be significantly more depleted than oxygen, as typically found in the inner solar system (Lee et al. 2010) and extrasolar planetesimals (Jura & Young 2014; Xu et al. 2014).

This simple snow line scenario for carbon/oxygen ratios is not universally valid. Anhydrous Interplanetary Dust Particles (IDPs), among the most primitive material in the solar system, are relatively carbon-rich and are thought to derive from comets despite their lack of hydrous minerals (Thomas et al. 1993). These anhydrous IDPs might therefore be related to those Kuiper Belt Objects (KBOs) such as Haumea (Lacerda & Jewitt 2007; Lockwood et al. 2014) and Eris (Sicardy et al. 2011) that are sufficiently dense to be no more than 15% ice by mass (Brown 2012) even though they likely contain large amounts of carbon. Here, we suggest that the minor planet being accreted onto Ton 345 is compositionally similar to an ice-poor KBO.

2. TON 345

Originally identified as a faint blue star at high galactic latitude, Ton 345 (= WD 0842+231) with $m(g) = 15.73$ mag in the Sloan Digital Sky Survey (SDSS) has an atmosphere composed almost entirely of helium. Ton 345 was singled out to be of special interest because it displays broad emission lines characteristic of a circumstellar gaseous disk orbiting within the tidal radius of the central white dwarf (Gaensicke et al. 2008). Subsequently, this star also has been found to have excess infrared emission produced by an orbiting dust disk (Brinkworth et al. 2012; Farihi et al. 2010; Melis et al. 2010). Experience has shown that at high spectral resolution, multiple elements can be detected in white dwarfs that display excess infrared emission, and we therefore obtained spectra at the Keck I telescope.

As listed by Xu et al. (2013), there are 4 well-studied white dwarfs with helium-dominated atmospheres, dust disks, and more than 10 elements heavier than He detected in their atmospheres: GD 362, GD 40, PG 1225-079, and WD J0738+1835, the only one to also display a gaseous component to its circumstellar disk. Here, we present results for Ton 345, an additional white dwarf with all of these distinctive characteristics.

3. OBSERVATIONS

The data reported here were acquired in 2008 at the Keck I telescope with HIRES (Vogt et al. 1994), an echelle spectrograph with a spectral resolution near 40,000. Table 4 of Melis et al. (2010) provides the exact exposure times and dates. In total, we obtained 6600 s and 9000 s of exposure time for the blue spectral range between 3130 Å and 5960 Å and the red spectral range between 4600 Å and 9000 Å, respectively.

The spectra were extracted from the flat-fielded two-dimensional image of each exposure as described in Klein et al. (2010, 2011). The most challenging task was removing the broad undulations in the continuum likely caused by variable vignetting (Suzuki et al. 2003). Also, as described in Klein et al. (2010), an additional re-normalizing processing step was

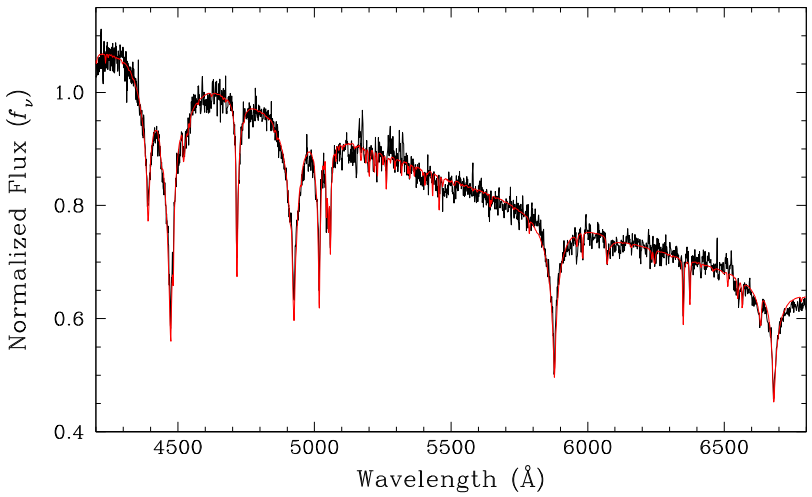

Figure 1. SDSS optical spectrum of Ton 345. Black denotes the data; the agreement of the He line profiles with the model denoted in red supports our inferred atmospheric parameters.

applied to calibrate and remove second (diffraction) order flux contamination in the region 8200–9000 Å. Wavelength calibration was performed using the standard Th-Ar lamps. Following Klein et al. (2010, 2011), we used IRAF to normalize the spectra and combine echelle orders.

With our signal to noise ratio which varied between 30 and 45, lines with an equivalent width as weak as 20 mÅ or even a little less can be detected. As a result, well over 100 lines from 11 elements heavier than helium are seen; there are no unidentified lines.

As noted by the referee, archived *Hubble Space Telescope* data acquired with the *Cosmic Origins Spectrograph* were acquired under program ID# 11561 with B. Gaensicke as PI. Although now available to the public, we have not included these data in our formal analysis. We did find that our model fit to the carbon and oxygen abundances derived from the HIRES spectra agree very well with the ultraviolet observations. However, because it is of great value to the scientific community to have independent abundance studies based on different data and model atmospheres, we have reported only analysis of the Keck observations.

4. ELEMENTAL ABUNDANCES

We first tried to estimate the atmospheric parameters by fitting the SDSS spectroscopic data with a grid appropriate for DB white dwarf stars. However, given that many of the helium lines are contaminated by metal absorption lines, we do not believe that the standard spectroscopic technique can provide accurate atmospheric parameters, especially for the surface gravity. We thus decided to instead obtain the effective temperature by fitting the *ugriz* photometry and keeping log g fixed at 8.0. We obtain $T_{\rm eff} = 19{,}535 \pm 700$ K. It is well known, however, that the presence of metals at the photosphere of a white dwarf can have a significant impact on the thermodynamic structure, leading to an overestimation of the effective temperature (Wegner & Koester 1985; Provencal et al. 2002; Dufour et al. 2005, 2010). We thus calculated a new DB grid with heavy elements assuming abundances close to our final adopted values. Fitting the ugriz data with this grid, we obtain, as expected, a lower effective temperature of 18,700 K ± 700 K, which we adopt for the rest of our analysis. Figure 1 shows a synthetic spectrum with these parameters over the SDSS data where most of the Si, Ca, and Fe lines are nicely reproduced, indicating that our assumptions were good and, most important, that the thermodynamic structure used for the rest of our analysis is more realistic. We also verified a posteriori that the measured abundances of lines from different ions (Mg I/Mg II and Fe I/Fe II) agreed very well (within 0.1 dex), indicating that the atmospheric parameters we have assumed are not significantly different than their true values.

Using the thermodynamic structure of a model calculated with $T_{\rm eff} = 18{,}700$ K, log $g = 8.0$, log H/He $= -5.0$, and the approximate amount of heavy elements discussed above, we next analyze the Keck observations following the procedure described in Dufour et al. (2012). The heavy element abundances found in this way were then used to compute a new model atmosphere

Table 1
Abundances in Ton 345

Element	[log n(Z)/n(He)]
H	$\leqslant -5.47$
C	−4.63 (0.19)
O	−4.58 (0.10)
Mg	−5.02 (0.10)
Al	−5.96 (0.10)
Si	−4.91 (0.12)
Ca	−6.23 (0.10)
Ti	−7.74(0.10)
Cr	−6.91 (0.10)
Mn	−7.54 (0.10)
Fe	−5.07 (0.10)
Ni	−6.20 (0.10)

Notes. In this table, we follow astronomical convention and report abundances by number. Key lines used in the abundance determinations include: Hα; C II 4267 Å, 6578 Å; O I 7771 Å, 7774 Å, 7775 Å; Mg I 3838 Å, 5184 Å; Mg II 7877 Å, 7896 Å; Al II 4663 Å, 6243 Å, 7042 Å, 7471 Å; Si II 3210 Å, 3854 Å, 3856 Å, 3863 Å, 4128 Å, 4131 Å, 5958 Å, Ca II 3159 Å, 3179 Å, 3181 Å, 3706 Å, 3737 Å, 3933 Å, 3968 Å; Ti II, Cr II, Fe II: multiple lines (Klein et al. 2010); Mn II 3442 Å, 3460 Å, 3474 Å; Ni II 3514 Å. Because only two lines are detected and only one with excellent signal to noise, the error for carbon is larger than for other elements. The hydrogen abundance is determined from the Hα proposal and is lower than employed in the model atmosphere used to compute abundances.

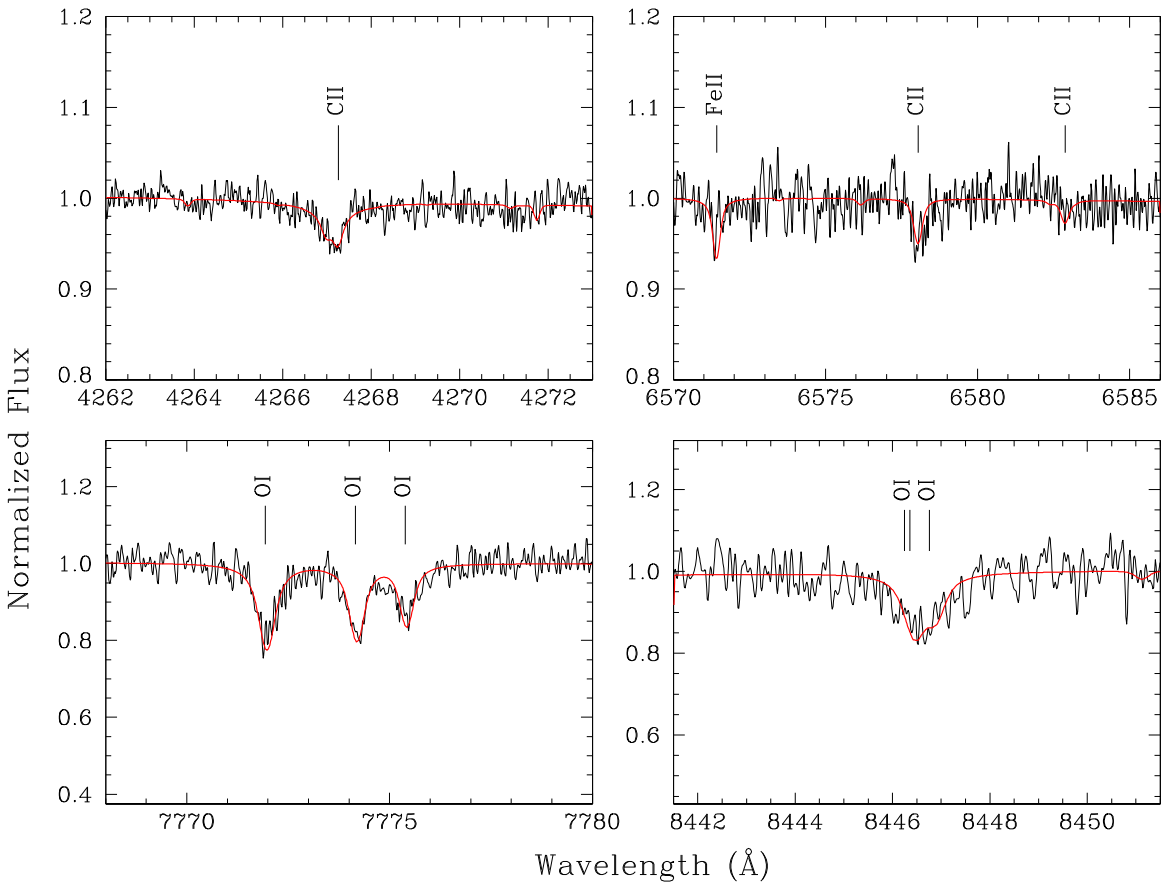

Figure 2. Spectrum of Ton 345 with lines of C, O, and Fe. Black denotes the data while red denotes the model with our inferred abundances. The model is wavelength shifted to the photospheric frame of the star; wavelengths are in air and the heliocentric frame of rest.

(we keep $T_{\rm eff}$ and log g fixed to the values cited above). We next repeat the fitting procedure using this new atmospheric structure and find that the abundances remain practically unchanged, indicating that we have converged to a final solution (see Table 1) and that no further iteration is required. Most of the lines are well separated from each other and therefore we can infer a value of an elemental abundance from an individual line. The dispersion in the various measurements for a given element can roughly be used as minimum abundance uncertainty, which is typically around 0.1 dex. For some elements, such as O, the dispersion of the abundances determined from individual lines can be as small as 0.02 dex. However, given the uncertainties in continuum placement, atomic parameters and the model atmosphere, we adopt a minimum error associated with each abundance determination of 0.1 dex. There are also uncertainties associated with the effective temperature and gravity, but, fortunately, the relative abundances are insensitive to small variations in these parameters (Klein et al. 2011). We show model fits to the spectral lines listed in Table 2 in Figures 2–9.

As far as we know, Ton 345 is the only externally polluted white dwarf to display optical carbon lines as seen in Figure 2. The carbon to oxygen ratio in Ton 345 is a factor of 10–1000 greater than found in other heavily polluted white dwarfs (Jura & Young 2014). The Hα line is at best only very marginally detected; we can only place an upper bound to the hydrogen abundance. Some of the Si II lines are not well fit; previous studies also have found difficulties in simultaneously fitting all available silicon lines in the spectra of externally polluted white dwarfs (Jura et al. 2012; Gaensicke et al. 2012).

Table 2
Percentage of Total Mass

Element	Ton 345 (%)	IDP (%)
C	15 (5.6)	12.5 (5.7)
O	23 (4.0)	32.9 (4.0)
Mg	13 (2.5)	10.7 (4.6)
Al	1.6 (0.36)	1.3 (1.1)
Si	19 (4.2)	14.6 (2.9)
Ca	1.3 (0.29)	0.9 (0.3)
Cr	0.35 (0.079)	0.2 (0.1)
Mn	0.086 (0.020)	0.2 (0.3)
Fe	26 (4.4)	17.6 (6.3)
Ni	2.0 (0.45)	0.7 (0.4)

Notes. Following cosmochemical convention, the abundances ratios are expressed by mass rather than by element number. The values for Ton 345 are derived from Table 1. Except for H and Ti whose abundances were not reported, the values for anhydrous IDPs in the third column are taken from Table 3 of Thomas et al. (1993) with their 1σ dispersion given in parentheses.

5. THE ACCRETED PARENT BODY

Because Ton 345 possesses a dust disk, it is likely that the pollution results from one large parent body with a well defined angular momentum vector; otherwise grains likely would be destroyed by mutual collisions (Jura 2008).

While dredge-up might enhance the carbon abundance in white dwarfs with effective temperatures near 25,000 K, this

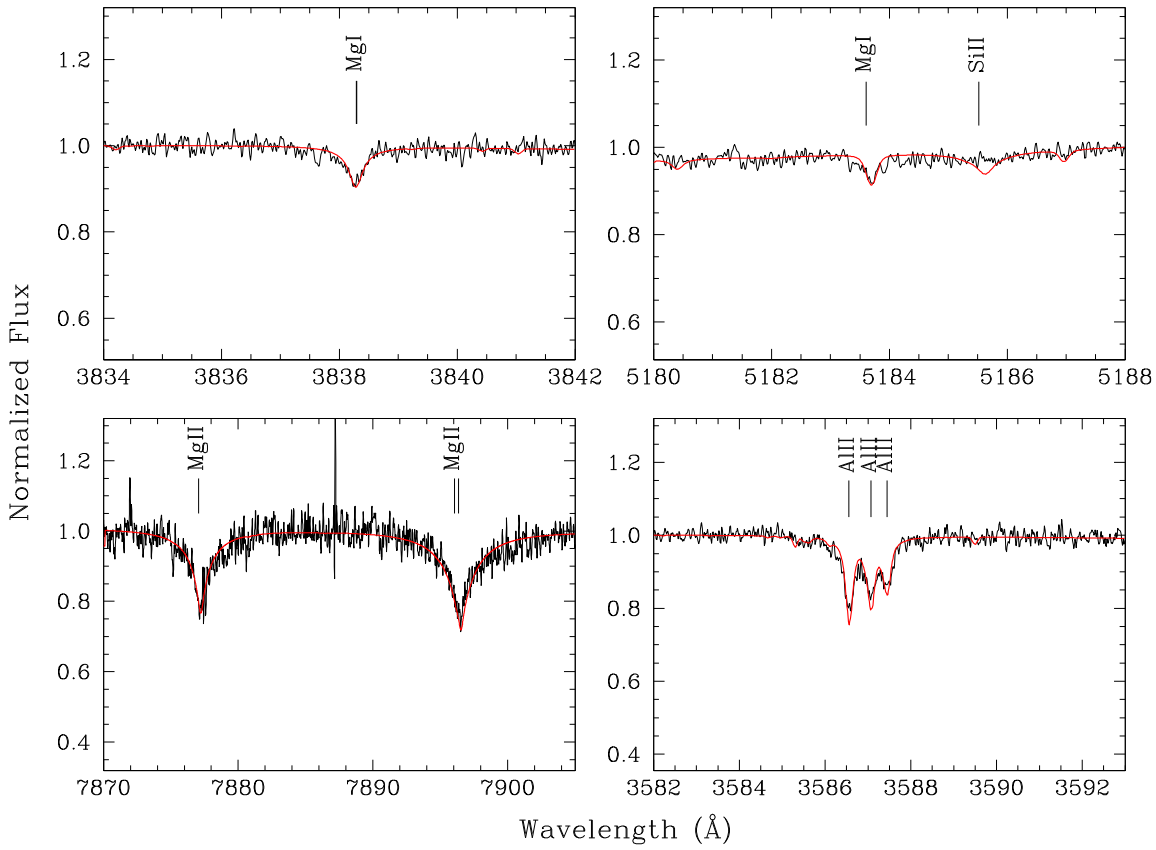

Figure 3. Same as Figure 2 with lines of Mg, Al, and Si.

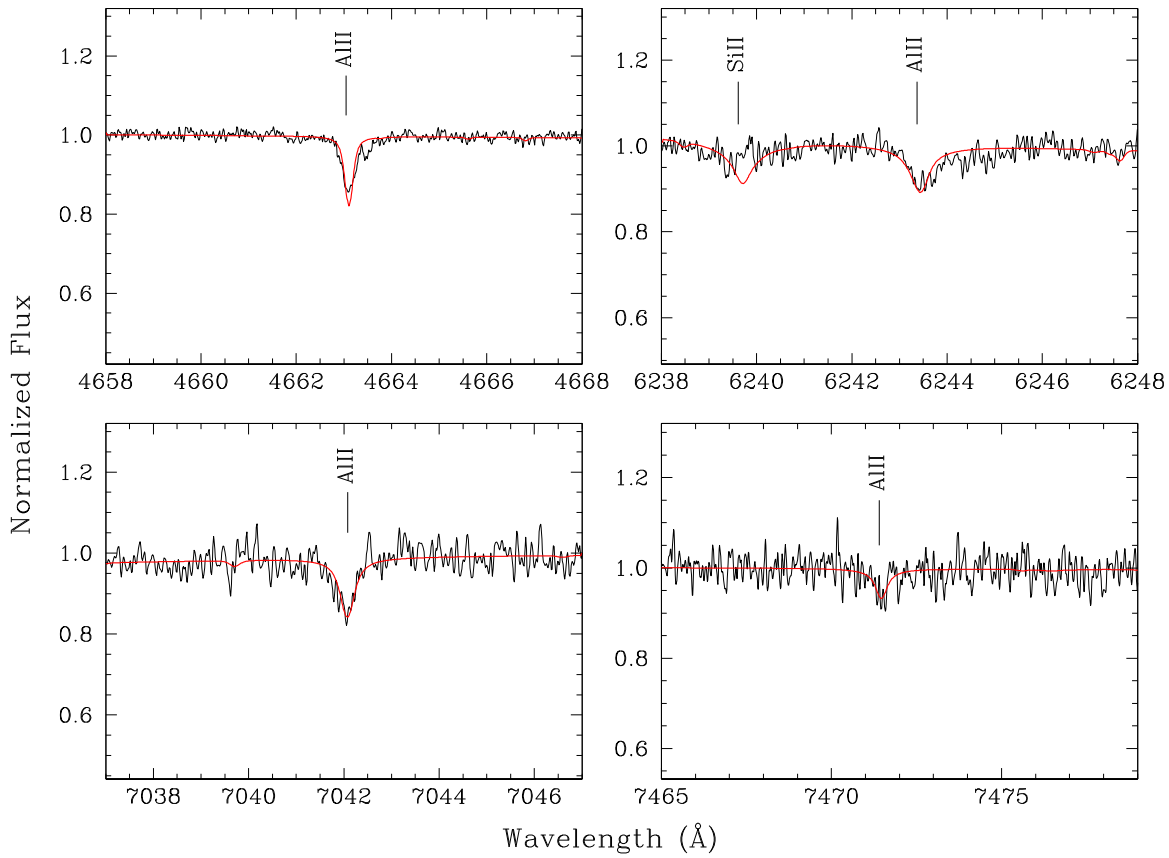

Figure 4. Same as Figure 2 with lines of Al and Si.

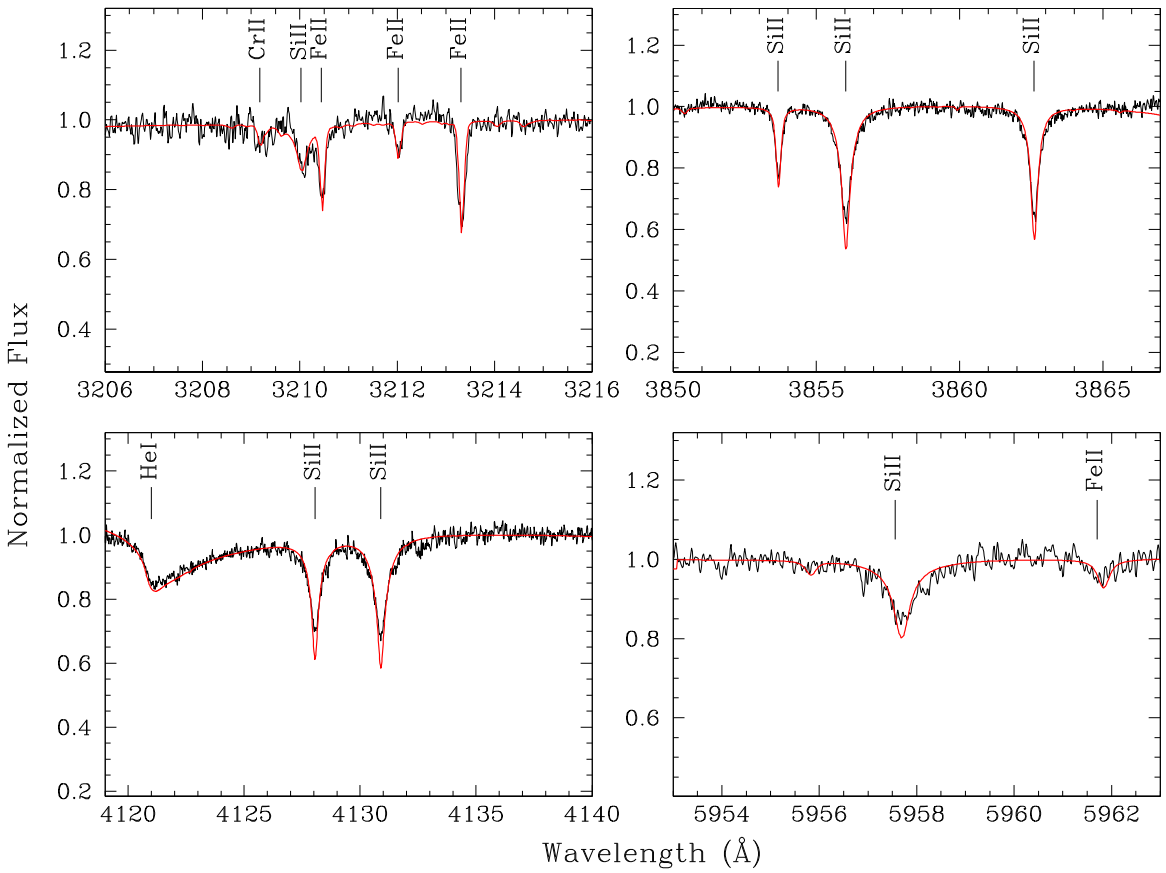

Figure 5. Same as Figure 2 with lines of He, Si, Cr, and Fe.

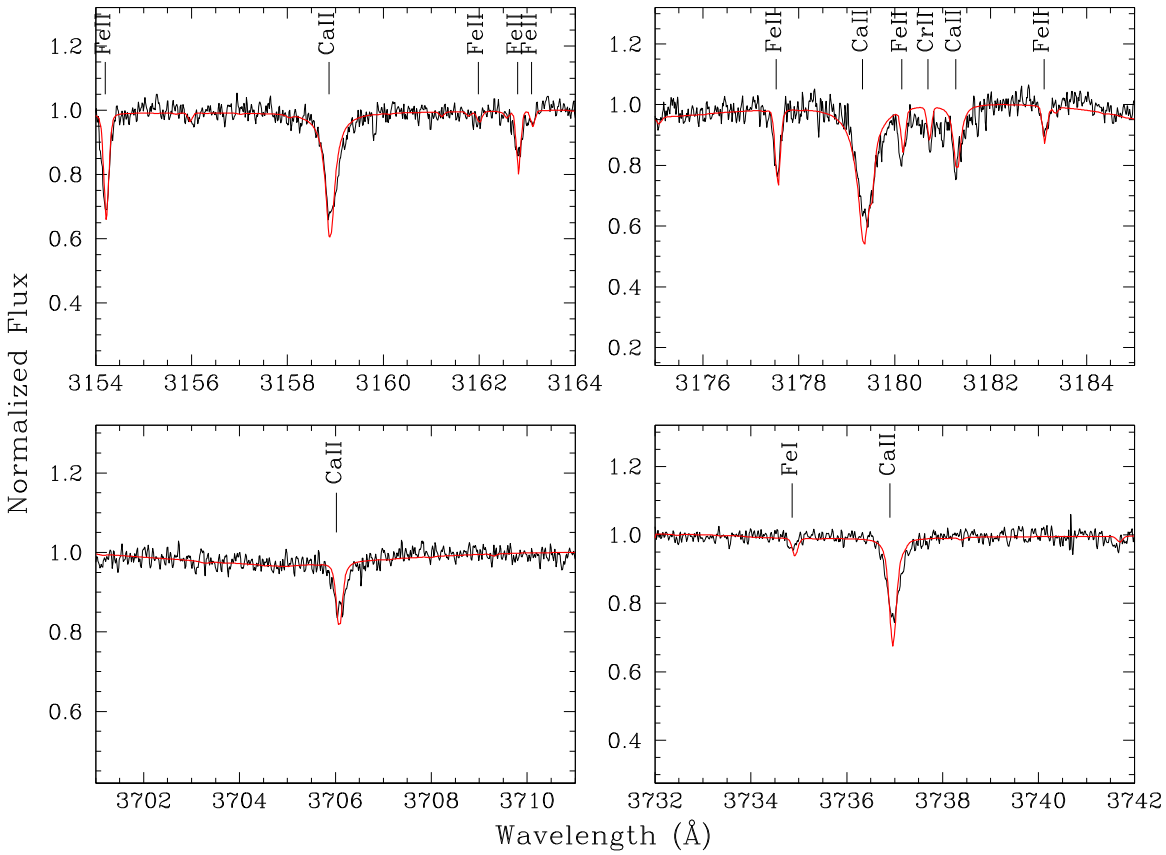

Figure 6. Same as Figure 2 with lines of Ca, Cr, and Fe.

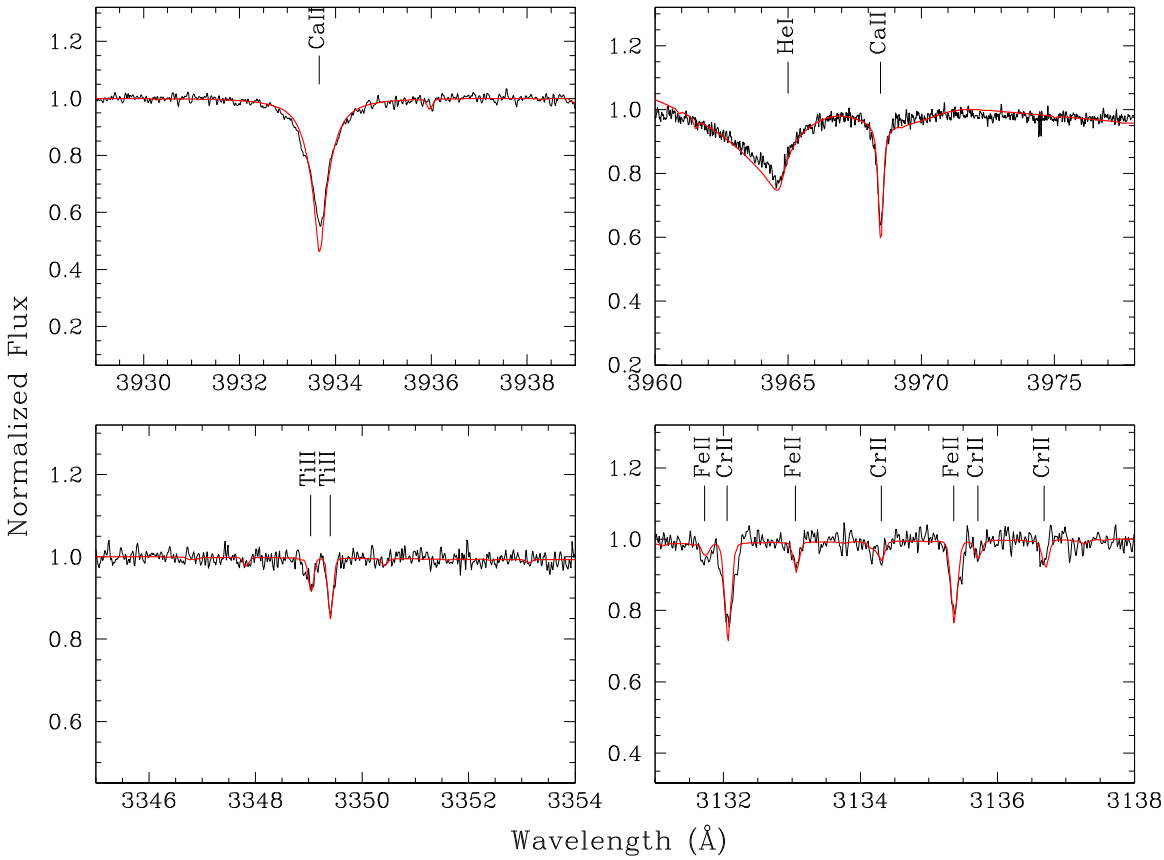

Figure 7. Same as Figure 2 with lines of He, Ca, Ti, Cr, and Fe.

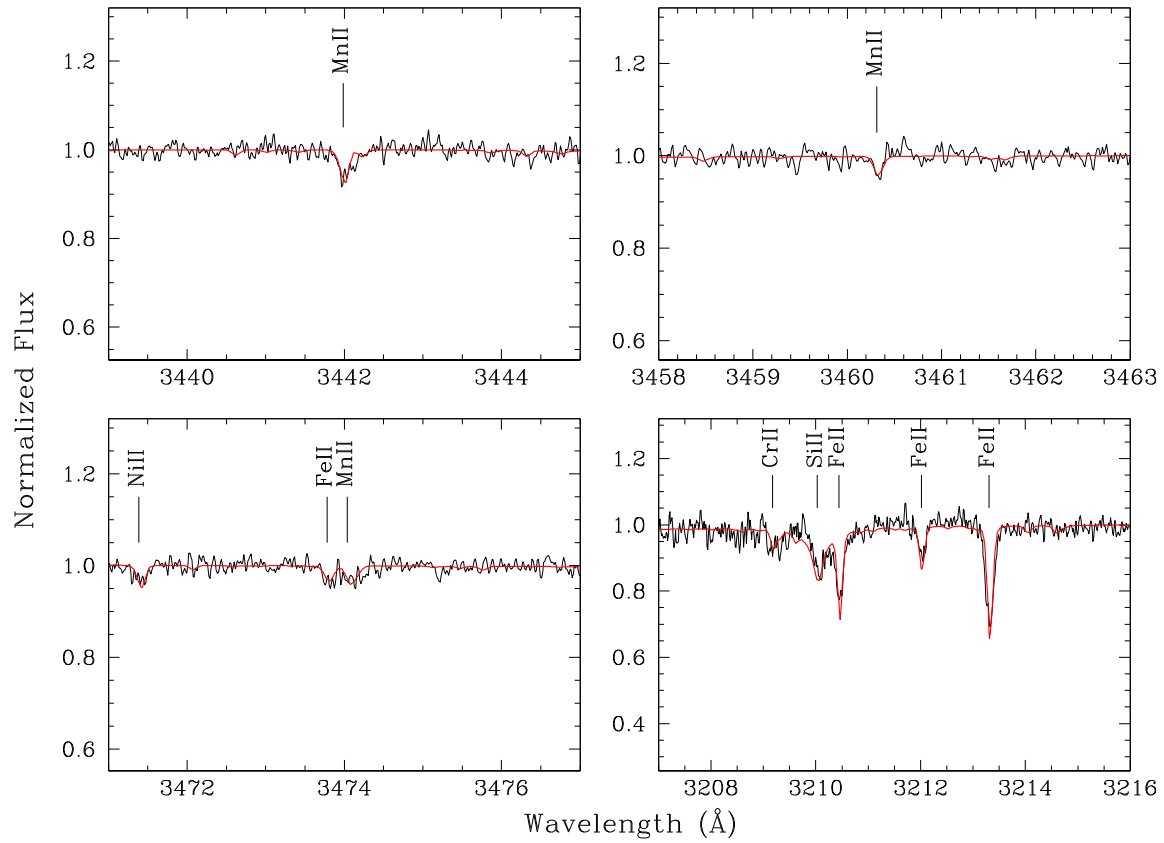

Figure 8. Same as Figure 2 with lines of Si, Mn, Cr, Fe, and Ni.

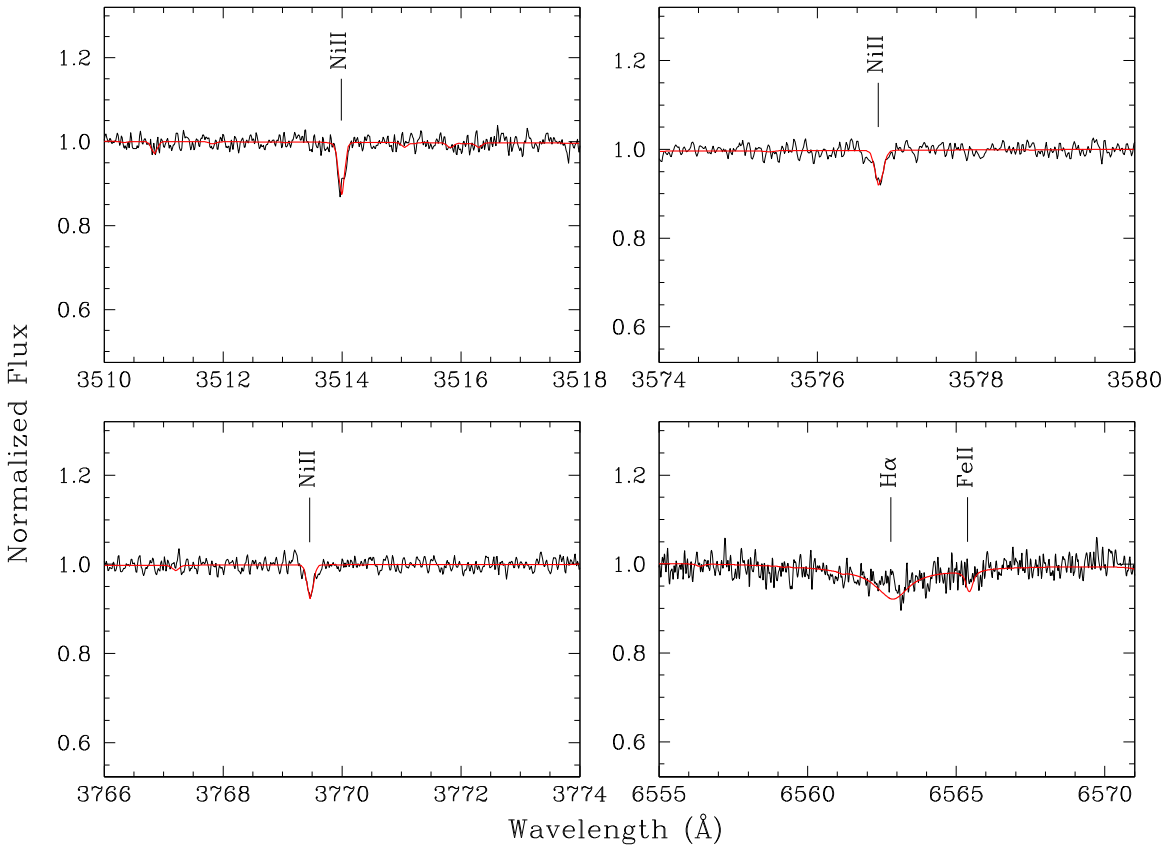

Figure 9. Same as Figure 2 except for selected lines of H, Fe, and Ni. The fit to Hα represents our upper bound to the abundance of this element which is only very marginally detected.

process is probably negligible for stars cooler than 20,000 K (Koester et al. 2014b). We therefore proceed by assuming that all of the heavy elements in the atmosphere of Ton 345 are accreted from its circumstellar disk.

Because different heavy elements settle at different rates, the abundances within the photosphere of an externally polluted white dwarf do not necessarily directly reflect the abundances in the parent body (Koester 2009). For Ton 345, the typical settling time[6] is 10^5 yr, comparable to estimates for the lower bound of a typical dust disk lifetime (Girven et al. 2012). Possibly, the outer convective zone might be in a steady state where the rate of accretion is balanced by the rate of gravitational settling. Alternatively, because it is both observed and theoretically predicted that accretion rates onto externally polluted white dwarfs can be variable on time scales much shorter than 10^5 yr (Metzger et al. 2012; Rafikov & Garmilla 2012; Wilson et al. 2014; Xu & Jura 2014), the abundances in the atmosphere of Ton 345 might reflect a recent burst of accretion.

Here, we assume the "instantaneous" approximation where the abundances in the photosphere equal the abundances in the parent body. If the system is in a steady state, the relative abundances of the lighter elements, C through Si, would be unchanged because their relative settling times differ by less than a factor of 1.2 from their mean value. In contrast, the relative abundances of the heavier elements such as Ca and Fe would increase by a factor of two. However, even though the fraction of the mass of the parent body mass carried in these heavy elements would be larger, our most important results—that carbon is unusually abundant and the material has little water, would be unaltered.

There are two arguments that the parent body accreted onto Ton 345 was anhydrous. If the matter accreted onto the white dwarf is carried within familiar minerals, then Mg, Al, Si, and Ca are bonded to oxygen in the proportions matching the oxides MgO, Al_2O_3, SiO_2, and CaO. Iron may be found either as an oxide or in metallic form. By this mineralogical argument, we find that all the oxygen is bound into minerals; none is left to form water. Also, the accreted minor planet was low in water because there is relatively little hydrogen in the atmosphere of Ton 345; from Table 1 and that most of the oxygen was bound in oxides, we compute that less than 10% of the oxygen was in the form of H_2O.

We now consider the composition of the accreted parent body. Using the abundances listed in Table 1, we compute the mass fraction of each element as provided in Table 2. Because of its large carbon abundance, it is possible that the planetesimal accreted onto Ton 345 resembles the most primitive meteorites, the C I chondrites. However, such a fit to our data is not very good, because C I chondrites have relatively more oxygen and less carbon then we measure in Ton 345. Among five well studied C I chondrites, the carbon mass percentage is 3.5% with a dispersion of 0.48% and a maximum value of 4.4% (Lodders 2003), much less than inferred for the material accreted onto Ton 345. Among the same five C I chondrites, the average oxygen mass percentage is 46%—with a dispersion of 5.8% and a minimum value of 41% (Lodders 2003)—is notably higher than our value of 23% inferred for the minor planet accreted onto Ton 345.

[6] Settling times are taken from http://www1.astrophysik.uni-kiel.de/~koester/astrophysics/.

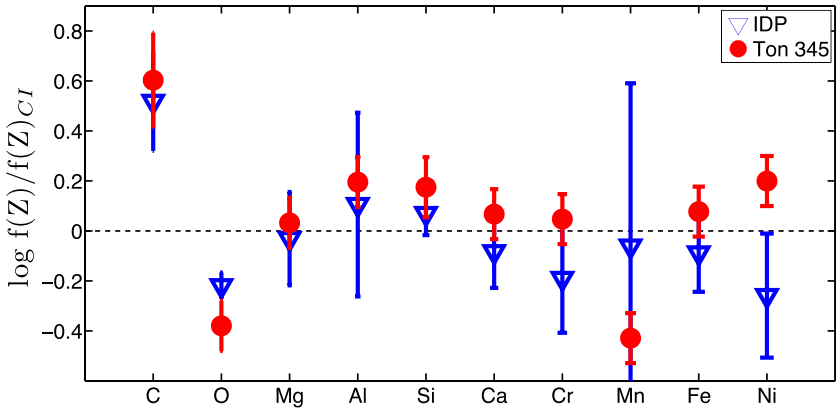

Figure 10. Comparison of the mass percentages in Ton 345 with those in anhydrous IDPs scaled to the average values in C I chondrites. We see that both the minor planet accreted onto Ton 345 and anhydrous IDPs are enriched in carbon and depleted in oxygen relative to C I chondrites.

Because of its high carbon to oxygen abundance ratio, the most familiar solar system material that matches the composition seen in Ton 345 is anhydrous IDPs, primitive matter whose average mass fractions (Thomas et al. 1993) also are given in Table 2. Approximately 50% of IDPs are anhydrous (Flynn et al. 2003), and these are the ones we consider here. The elemental mass fractions for Ton 345's pollution and of anhydrous IDPs agree except for Ni.

For our model atmosphere, we compute that the He mass in the outer convection zone is 9.1×10^{25} g. Consequently, from the abundances given in Table 1, the total mass of the accreted parent body must have been at least 1.6×10^{23} g, about 60% of the mass of Vesta (Russell et al. 2012). If its density was 3 g cm^{-3}, then the parent body diameter was at least 470 km, well within the range inferred for these parameters for extrasolar planetesimals accreted onto heavily polluted white dwarfs (Jura & Young 2014).

6. DISCUSSION

Previous observations have shown extrasolar minor planets accreted by white dwarfs typically have little water (Jura & Xu 2012), although the parent body accreted onto GD 61 is an exception in being water-rich (Farihi et al. 2013). In contrast, the object accreted onto Ton 345 is relatively carbon-rich and water-poor, indicating that the carbon to water content in extrasolar minor planets varies by more than a factor of 1000.

A star's C/O ratio influences the carbon and water content of planetesimals that are formed in its protoplanetary nebulae (Johnson et al. 2012). However, essentially all main sequence stars near the Sun have approximately solar oxygen and carbon abundances (Fortney 2012; Nissen 2013; Teske et al. 2014) and the observed range in the carbon to oxygen ratio among externally polluted white dwarfs must be largely a consequence of substantial separation of these two elements during formation and evolution.

Heavily polluted white dwarfs with dust disks typically have low carbon abundances (Jura & Young 2014). In contrast, some white dwarfs with relatively modest levels of heavy element pollution and with only C and Si abundances reported (Koester et al. 2014b) have notably higher carbon to silicon abundance ratios than do systems where abundances of multiple elements have been found. One possible explanation for the pollution with relatively high carbon abundance is that the parent bodies originate in the outer planetary system. However, we do not yet have a full understanding of the cosmochemical evolution of carbon in extrasolar planetary systems.

Because we have measured abundances of 11 heavy elements in the atmosphere of Ton 345, we can constrain many potential scenarios for the origin of the accreted minor planet accreted. Brown (2012) has suggested that high-density KBOs with relatively little water are the consequence of the collisional erosion of a differentiated parent body which had an ice shell and a rocky core. Because differentiation is widespread among extrasolar planetesimals (Jura et al. 2013), some related model may pertain to the minor planet accreted onto Ton 345. We show in Figure 10 a comparison between the mass fractions listed in Table 2 for Ton 345 and those for an anhydrous IDP, normalized to the abundances in C I chondrites. The good agreement can be understood as being the consequence of the evolution of a differentiated minor planet which initially had an ice exterior. At some later time, all the exterior ice was lost either by a collision or some other process such as sublimation during the star's highly luminous red giant phase before it became a white dwarf (Jura 2004). Buried water ice could be retained (Jura & Xu 2010). Regardless of how this hypothetical differentiated planetesimal lost its outer ice, ultimately, it would achieve a bulk composition resembling those solar system KBOs with relatively high density and little water.

7. CONCLUSIONS

We have obtained optical spectra of Ton 345 and measured the abundances of 11 elements heavier than helium. We find that we are observing the disintegration of a minor planet that likely was carbon-rich and ice-poor; it appears to have been compositionally similar to a high density KBO.

This work has been partly supported by the NSF. We thank M. Nabeshima for help with the data analysis.

REFERENCES

Bergin, E. A. 2013, in AIP Conf. Proc., XVII Special Courses at the National Observatory of Rio de Janeiro (Melville, NY: AIP), arXiv:1309.4729
Bonsor, A., Mustill, A. J., & Wyatt, M. C. 2011, MNRAS, 414, 930
Brinkworth, C. S., Gaensicke, B. T., Girven, J. M., et al. 2012, ApJ, 750, 86
Brown, M. E. 2012, AREPS, 40, 467
Debes, J. H., & Sigurdsson, S. 2002, ApJ, 572, 556
Dufour, P., Bergeron, P., & Fontaine, G. 2005, ApJ, 627, 404
Dufour, P., Kilic, M., Fontaine, G., et al. 2010, ApJ, 719, 803
Dufour, P., Kilic, M., Fontaine, G., et al. 2012, ApJ, 749, 6
Farihi, J., Gaensicke, B. T., & Koester, D. 2013, Sci, 342, 218

Farihi, J., Jura, M., Lee, J.-E., & Zuckerman, B. 2010, ApJ, 714, 1386
Flynn, G. J., Keller, L. P., Feser, M., Wirick, S., & Jacobsen, C. 2003, GeCoA, 67, 479
Fortney, J. 2012, ApJL, 747, L27
Frewen, S. F. N., & Hansen, B. M. S. 2014, MNRAS, 439, 2442
Gaensicke, B. T., Koester, D., Farihi, J., et al. 2012, MNRAS, 424, 333
Gaensicke, B. T., Koester, D., Marsh, T. R., Rebassa-Mansergas, A., & Southworth, J. 2008, MNRAS, 391, L103
Girven, J., Brinkworth, C. S., Farihi, J., et al. 2012, ApJ, 749, 154
Henning, T., & Semenov, D. 2013, ChRv, 113, 9016
Johnson, T. V., Mousis, O., Lunine, J., & Madhusudhan, N. 2012, ApJ, 757, 192
Jura, M. 2003, ApJL, 584, L91
Jura, M. 2004, ApJ, 603, 729
Jura, M. 2008, AJ, 135, 1785
Jura, M., & Xu, S. 2010, AJ, 140, 1129
Jura, M., & Xu, S. 2012, AJ, 143, 6
Jura, M., Xu, S., Klein, B., Koester, D., & Zuckerman, B. 2012, ApJ, 750, 69
Jura, M., Xu, S., & Young, E. D. 2013, ApJL, 775, L41
Jura, M., & Young, E. D. 2014, AREPS, 42, 45
Klein, B., Jura, M., Koester, D., & Zuckerman, B. 2011, ApJ, 741, 64
Klein, B., Jura, M., Koester, D., Zuckerman, B., & Melis, C. 2010, ApJ, 709, 950
Koester, D. 2009, A&A, 498, 517
Koester, D., Gaensicke, B., & Farihi, J. 2014a, A&A, 566, 34
Koester, D., Provencal, J., & Gaensicke, B. T. 2014b, A&A, 568, 118
Lacerda, P., & Jewitt, D. C. 2007, AJ, 133, 1393
Lee, J.-E., Bergin, E. A., & Nomura, H. 2010, ApJL, 710, L21
Lockwood, A. C., Brown, M. E., & Stansberry, J. 2014, EM&P, 111, 127
Lodders, K. 2003, ApJ, 591, 1220
Melis, C., Jura, M., Albert, L., Klein, B., & Zuckerman, B. 2010, ApJ, 722, 1078
Metzger, B. D., Rafikov, R. R., & Bochkarev, K. V. 2012, MNRAS, 423, 505
Nissen, P. E. 2013, A&A, 552, 73
Provencal, J. L., Shipman, H. L., Koester, D., Wesemael, F., & Bergeron, P. 2002, ApJ, 568, 324
Rafikov, R. R., & Garmilla, J. A. 2012, ApJ, 760, 123
Russell, C. T., Raymond, C. A., Coradini, A., et al. 2012, Sci, 336, 684
Sicardy, B., Ortiz, J. L., Assafin, M., et al. 2011, Natur, 478, 493
Suzuki, N., Tytler, D., Kirkman, D., O'Meara, J. M., & Lubin, D. 2003, PASP, 115, 1050
Teske, J. K., Cunha, K., Smith, V. V., Schuler, S. C., & Griffith, C. A. 2014, ApJ, 788, 93
Thomas, K. L., Blanford, G. E., Keller, L. P., Klock, W., & McKay, D. S. 1993, GeCoA, 57, 1551
Veras, D., & Wyatt, M. C. 2012, MNRAS, 421, 2969
Vogt, S. S., Allen, S. L., Bigelow, B. C., et al. 1994, Proc. SPIE, 2198, 362
Wegner, G., & Koester, D. 1985, ApJ, 288, 746
Wilson, D. J., Gaensicke, B. T., Koester, D., et al. 2014, MNRAS, 445, 1878
Xu, S., & Jura, M. 2014, ApJL, 792, L39
Xu, S., Jura, M., Klein, B., Koester, D., & Zuckerman, B. 2013, ApJ, 766, 132
Xu, S., Jura, M., Koester, D., Klein, B., & Zuckerman, B. 2014, ApJ, 783, 79